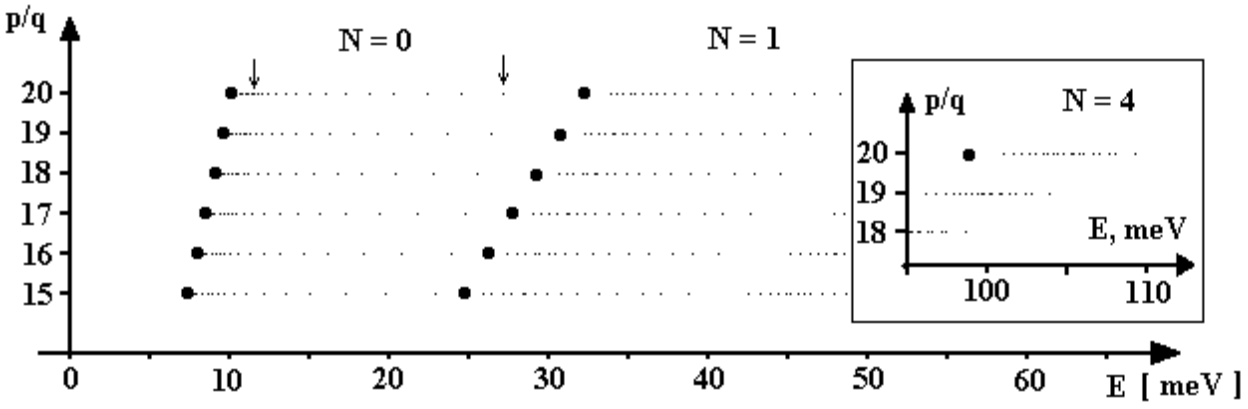
p/q
N = 0
N = 1
20
19
18
17
16
15
0
10
20
30
40
50
60
E [meV]
p/q
N = 4
20
19
18
E, meV
100
110

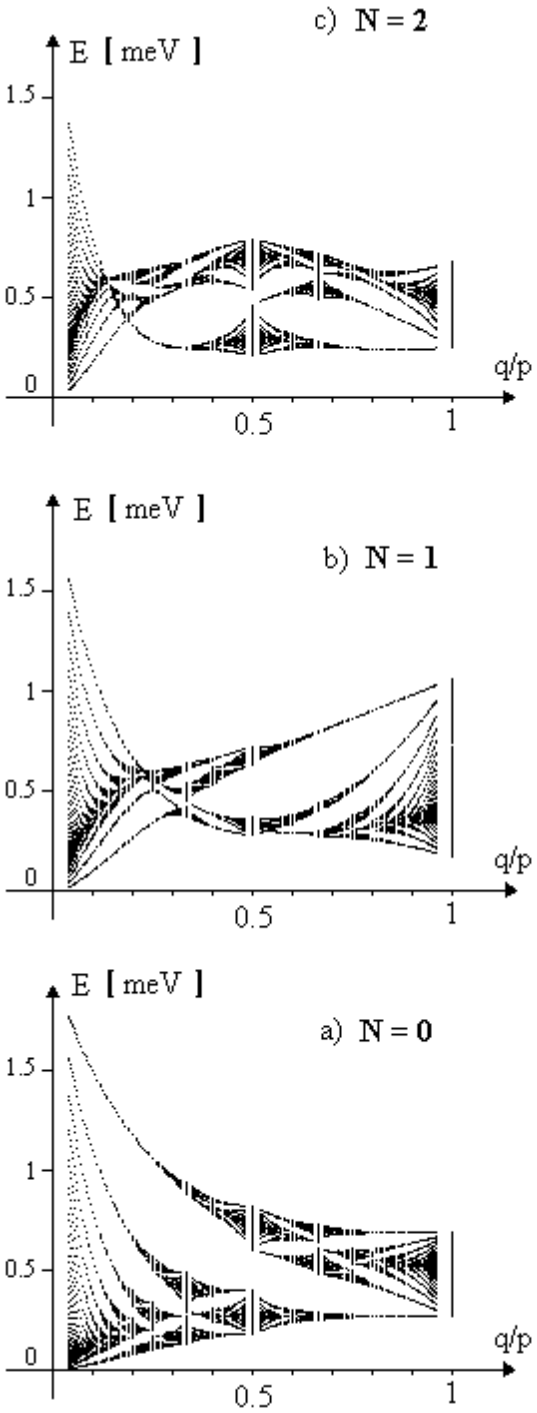
c) N = 2
E [meV]
1.5
1
0.5
0
q/p
0.5
1
E [meV]
b) N = 1
1.5
1
0.5
0
q/p
0.5
1
E [meV]
a) N = 0
1.5
1
0.5
0
q/p
0.5
1

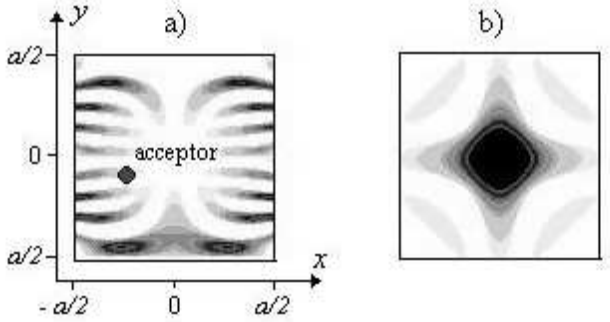
a)
b)
y
x
a/2
0
a/2
- a/2
0
a/2
acceptor

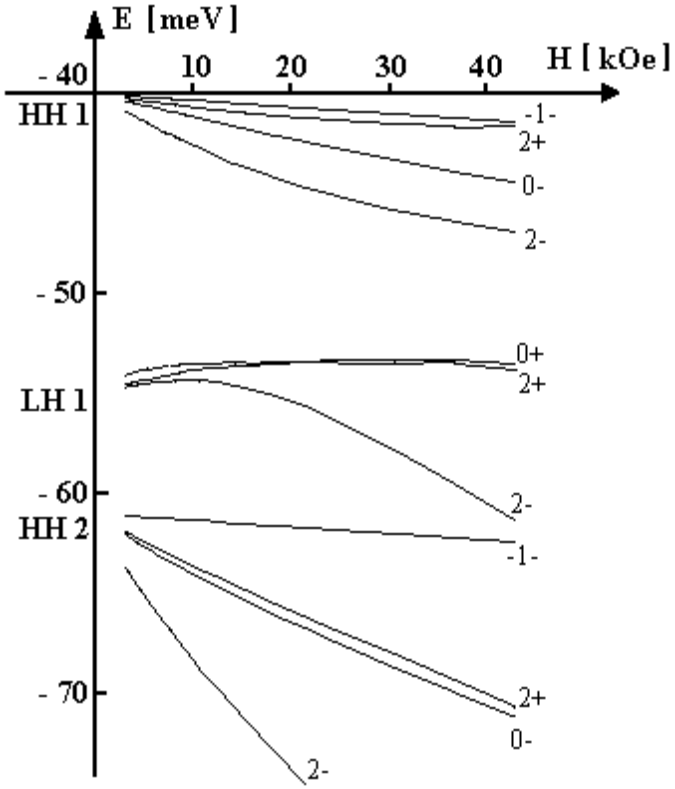
E [meV]
H [kOe]
10
20
30
40
- 40
- 50
- 60
- 70
HH 1
LH 1
HH 2
-1-
2+
0-
2-
0+
2+
2-
-1-
2+
0-
2-

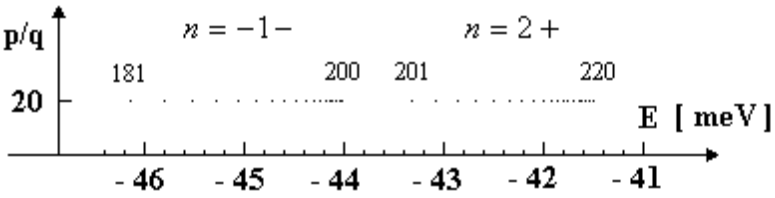
p/q
n = −1−
n = 2 +
181
200
201
220
20
E [meV]
- 46
- 45
- 44
- 43
- 42
- 41

b) $n = 0+$

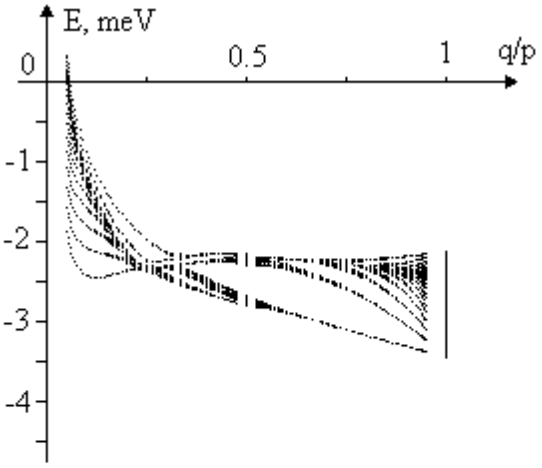

a) $n = 0-$

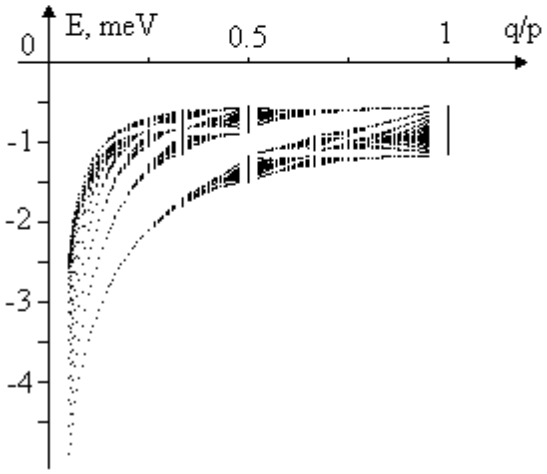

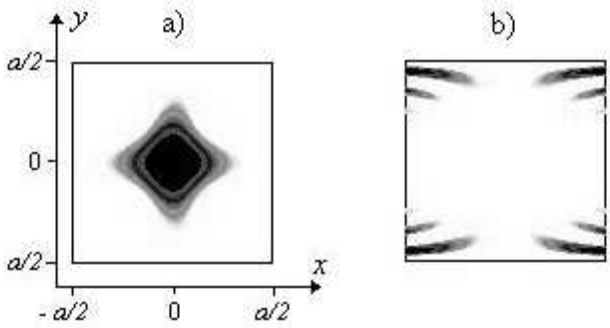
a)
b)
y
x
a/2
0
a/2
- a/2
0
a/2

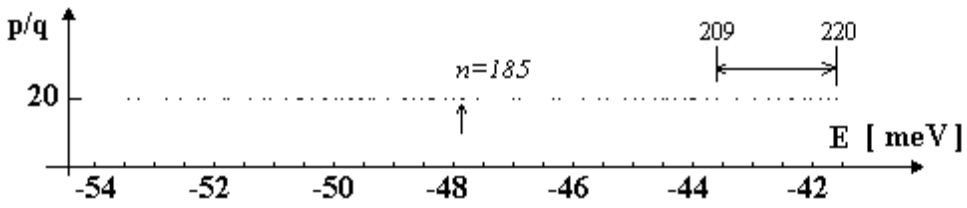
p/q
20
n=185
209
220
E [meV]
-54
-52
-50
-48
-46
-44
-42

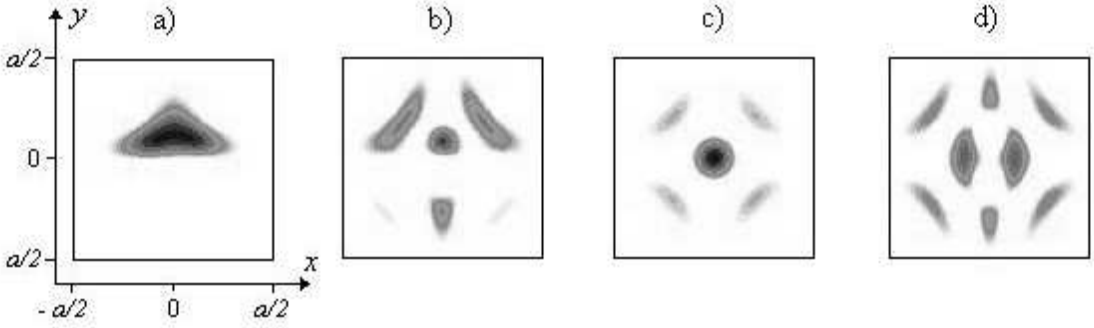
a)
b)
c)
d)
y
x
a/2
0
a/2
- a/2
0
a/2

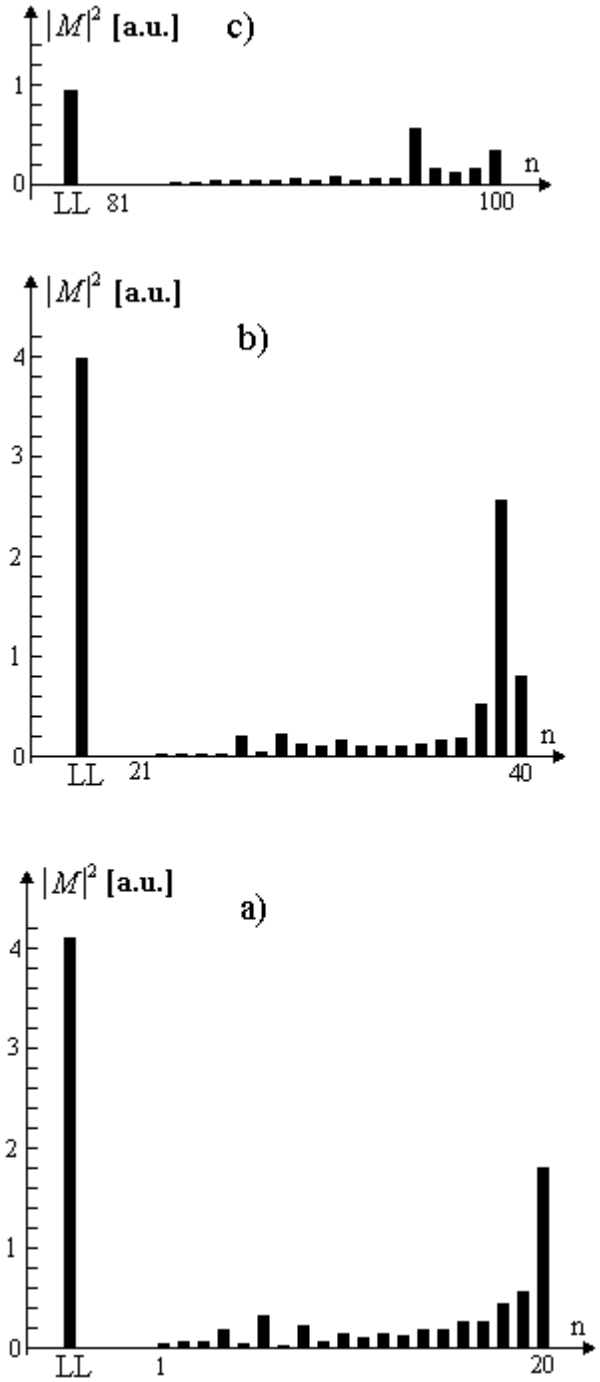
|M|² [a.u.]
c)
1
0
LL
81
100
n
|M|² [a.u.]
b)
4
3
2
1
0
LL
21
40
n
|M|² [a.u.]
a)
4
3
2
1
0
LL
1
20
n

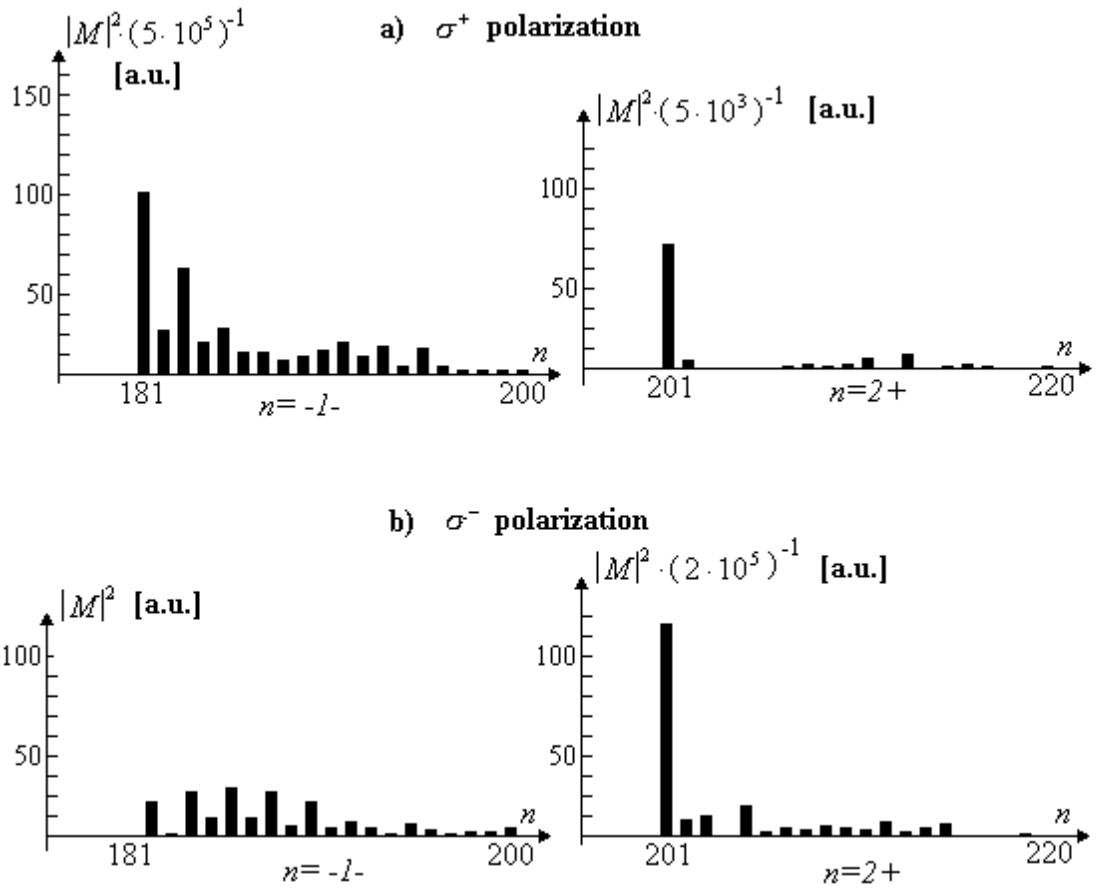
a) σ+ polarization
|M|²·(5·10⁵)⁻¹ [a.u.]
150
100
50
181
n= -1-
200
n
|M|²·(5·10³)⁻¹ [a.u.]
100
50
201
n=2+
220
n
b) σ− polarization
|M|² [a.u.]
100
50
181
n= -1-
200
n
|M|²·(2·10⁵)⁻¹ [a.u.]
100
50
201
n=2+
220
n

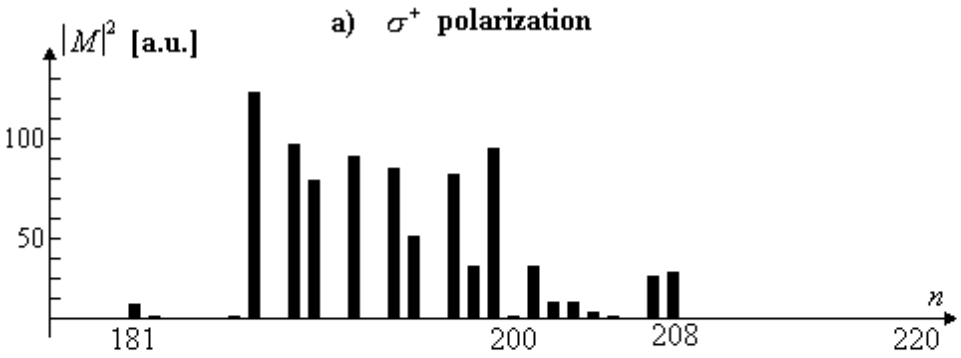
a) σ^+ polarization
$|M|^2$ [a.u.]
100
50
n
181
200
208
220

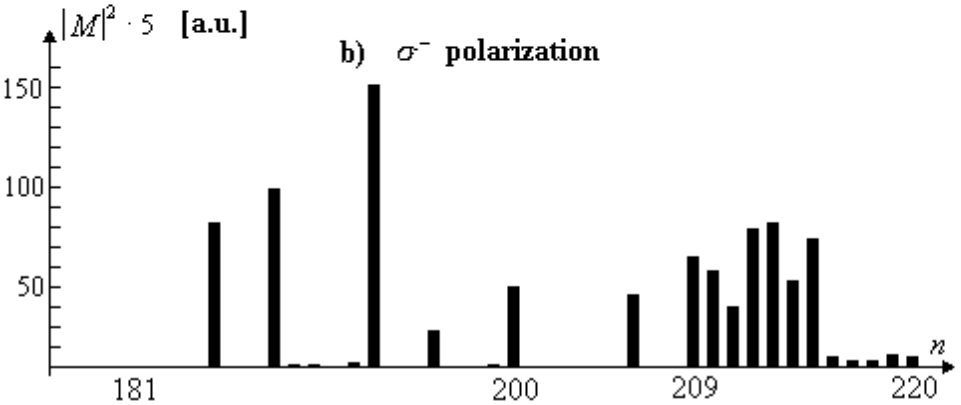
$|M|^2 \cdot 5$ [a.u.]
b) σ^- polarization
150
100
50
n
181
200
209
220

arXiv:cond-mat/0112465v1 [cond-mat.mes-hall] 27 Dec 2001

Quantum states and optics in n - and p -type heterojunctions with lateral surface quantum dot (antidot) superlattice subjected to perpendicular magnetic field

V.Ya. Demikhovskii * and D.V. Khomitsky
Nizhny Novgorod State University
Gagarin Ave. 23, Nizhny Novgorod 603950, Russia

The studies of quantum states and optics in n- and p-type heterojunctions with lateral surface quantum dot (antidots) superlattice and in the presence of perpendicular magnetic field are performed. The Azbel' – Hofstadter problem is solved for electrons in conduction band and for holes in valence band described by 4×4 Luttinger Hamiltonian. Under the conditions of non-interactive Landau levels the set of magnetic subbands is obtained for separate electron and hole levels in wide interval of magnetic field. The influence of spin-orbit interaction onto wavefunctions and energy spectrum in hole magnetic subbands has been investigated. The probabilities of transitions between quantum states in magnetic subbands and monolayer of impurities located inside heterojunction are calculated for two cases: transitions between electron states and acceptors and between hole states and donors. The set of parameters (superlattice periods, amplitude of periodic potential and magntitude of magnetic field, etc.) required for experimental observation of magnetic subbands is found.

PACS number(s): 73.21.-b, 73.21 Cd, 78.67.-n

I. INTRODUCTION

The problem of quantum states of 2D Bloch electrons subjected into magnetic field remains actual over several last decades. The fascinating physical phenomena occuring here are caused by interaction of lattice periodic potential which leads to band structure of spectrum with vector potential of uniform magnetic field tending to form discrete energy levels. The crucial parameter determining the nature of quantum states in this problem is a magnetic flux through lattice elementary cell. If this flux equals rational number p/q of flux quanta $\Phi_0 = 2\pi\hbar c/|e|$ (p and q are mutual prime integers), the magnetic translations form a group. In this case it becomes possible to determine the transformational law for wavefunction under translations, the magnetic Brillouin zone and the subband energy spectrum. When the amplitude of periodic potential V_0 is smaller then cyclotron energy $\hbar\omega_c$ one can neglect the influence of neighbouring Landau levels and may obtain the set of magnetic subbands arising from single level[1]. In this scheme every Landau level splits into p subbands with degeneracy degree q. If it becomes needful to include the interaction between Landau levels, numerical methods are usually applied for calculation of quantum states[2–4].

During last years several significant theoretical aspects of discussed problem have been investigated. In particular, quantization of Hall conductance in the presence of additional periodic potential has been studied in[1,3,5]. One might expect that each of magnetic subbands to give a Hall conductance equal to e^2/ph, but according to Laughlin each subband must carry an integer multiple of the Hall current carried by the entire Landau level. The analytical approaches applied in[6–8] have indicated that the problem of Bloch quantum states in magnetic field can be studied using the methods of Bethe - Ansatz. In particular, the "mid" band spectrum of the model and the Bloch wavefunction can be found analytically from Bethe - Ansatz equation that is typical for

*demi@phys.unn.runnet.ru

completely integrable quantum systems. In more complicated models describing Bloch electrons in magnetic field the manifestation of quantum chaos has been discovered[9–11].

Recently the number of experimental studies have been performed in order to investigate electron quantum states in 2D heterojunctions with lateral surface superlattice of quantum dots (abtidots). Such a system is convenient for investigation of both classical effects (commensurability of lattice periods and cyclotron radius, transition to chaos, etc.) and of energy spectrum consisting of magnetic subbands. For example, in[9,12] the oscillations of longitude magnetoresistance have been detected under the conditions where classical cyclotron radius $2R_c$ envelopes the integer number of antidots or numerous reflections from one antidot occur. The first experimental evidences of Landau levels splitted into the set of magnetic subbands have been obtained in[13] by longitude magnetoresistance studies. Then, the measurements of Hall resistance in subband energy spectrum have also been performed and reportered this year[14].

Besides the magnetoresistance measurements, the attempts of magnetooptical studies of interband transitions between conduction band and acceptor impurities[15] have been performed in n -type heterostructures. The experiments in p-type heterojunctions without periodic potential have also become possible due to the progress in technology which substantially improved the quality of the p channels in GaAs/AlGaAs heterojunctions[16]. Thus, almost all intriguing phenomena found for 2D electron system were also observed in 2D hole channels. The specific traits of hole quantum states which have caused the interest to them may be briefly described as non-trivial effects of symmetry and spin-orbit interaction. It is known that in the absence of magnetic field the electron spectrum in symmetrical quantum well is twofold degenerate with respect to spin. On the opposite, in asymmetrical heterojunction grown, for example, in z direction where $V(z) \neq V(-z)$ the relativistic orbital interaction of electron magnetic moment and macroscopic heterojunction potential leads to the breakdown of spin degeneracy. Only twofold Kramers degeneracy $E(\mathbf{k}, \uparrow) = E(-\mathbf{k}, \downarrow)$ remains.

In order to obtain transparent and valuable results from transport and optical experiments, one may need to choose the set of parameters (superlattice periods, value of magnetic field and amplitude of periodic potential, etc.) which provide a sharp, easily distinguishable picture of non-overlapped magnetic subbands originating from particular Landau level. Such energy spectra and wavefunctions are studied in the present paper together with calculation of matrix elements for interband transitions between magnetic subbands and impurities. In Sec. II we obtain electronic spectra and wavefunctions for spinless electrons in n-type heterojunction with lateral superlattice of quantum antidots and perpendicular magnetic field. In this case we assume a simple parabolic electron spectrum and here it is possible to neglect spin-orbit coupling. Sec. III is devoted to the studies of hole quantum states in p-type heterojunction subjected to magnetic field (Subsec. IIIA) and both to magnetic field and periodic potential of quantum dots superlattice (Subsec. IIIB). On the opposite to the case of electron states, the spin-orbit coupling is included here which is principal for description of holes in semiconductors. We calculate hole magnetic subbands and wavefunctions assuming several levels of size quantization in heterojunction. Then in Sec. IV we calculate the matrix elements for transitions between electron magnetic subbands and monolayer of acceptors located inside heterojunction, and for transitions between hole magnetic subbands and monolayer of donors. The huge difference in magnitude of matrix elements corresponding to different magnetic subbands was found and the dependence of transition probabilities on polarization was investigated. These results may be used for identification of complicated magnetic subband spectra in magnetooptical experiments. The summary of our results is given in Sec. V.

II. ELECTRON STATES IN HETEROJUNCTION WITH LATERAL SUPERLATTICE AND PERPENDICULAR MAGNETIC FIELD

The Bloch electron wavefunction at the Γ-point of conduction band of n-type GaAs/AlGaAs heterojunction can be constructed in envelope function approximation as a product of s - type atomic function $s(\mathbf{r})$ and envelope function $\psi_{k_x k_y}$:

$$\Psi_{k_x k_y}(\mathbf{r}) = \psi_{k_x k_y} s(\mathbf{r}). \tag{1}$$

In Eq.(1) $\psi_{k_x k_y}$ stands for envelope function which satisfies to Schrödinger equation for spinless electron with effective mass m_{eff} subjected into uniform magnetic field $\mathbf{H}||Oz$ and periodic potential of lateral surface superlattice which can be chosen in the form[4]

$$V(x,y) = V_0 \cos^2 \frac{\pi x}{a} \cos^2 \frac{\pi y}{a}. \tag{2}$$

Here a is superlattice period and the case $V_0 < 0$ (> 0) corresponds to periodic electric potential generated by quantum dots (antidots) superlattice. The Bloch electron wavefunction $\psi_{k_x k_y}$ which is the solution of Schrödinger equation with vector potential

$$\mathbf{A} = (0, Hx, 0) \tag{3}$$

and periodic potential (2) satisfies to the generalized Bloch boundary conditions (Peierls conditions)

$$\psi_{k_x k_y}(x,y,z) = \psi_{k_x k_y}(x+qa, y+a, z) \exp(-ik_x qa) \times \\ \times \exp(-ik_y a) \exp(-2\pi i p y/a), \tag{4}$$

In Eq.(4) the magnetic flux $\Phi = Ha^2$ through superlattice elementary cell equals rational number p/q of flux quanta $\Phi_0 = 2\pi\hbar c/e$ where p and q are mutually prime integers. Following[4], we write the electron wavefunction as

$$\psi_{k_x k_y}(\mathbf{r}) = \frac{1}{La\sqrt{q}} \sum_{N=0}^{\infty} \sum_{n=1}^{p} C_{Nn}(k_x,k_y) \sum_{l=-L/2}^{L/2} u_N \left(\frac{x - x_0 - lqa - nqa/p}{\ell_H} \right) \times \\ \times \exp\left(ik_x \left[lqa + \frac{nqa}{p} \right] \right) \exp\left(2\pi i y \frac{lp+n}{a} \right) \exp(ik_y y) \tag{5}$$

where $\ell_H = \sqrt{\hbar c/eH}$ is a magnetic length, $x_0 = k_y \ell_H^2$ and $u_N(x)$ is N-th harmonic oscillator wavefunction. We substitute wavefunction (5) into Scrödinger equation and after standard quantum-mechanical projection onto basis in Hilbert space the eigenvalue problem for coefficients C_{Nn} is obtained. The energy spectrum $\varepsilon_{Nn}(k_x,k_y)$ forms a set of p magnetic subbands ($n = 1, \ldots, p$) for each Landau level N[1]. Electron spectrum at $k_x = k_y = 0$ in antodot lattice with $a = 80\ nm$ and $V_0 = 20\ meV$ is shown on Fig.1 for three Landau levels: $N = 0$, $N = 1$, and for $N = 4$ on the inset. At high magnetic fields when $\hbar\omega_c > V_0$ these subbands are very narrow and look like a set of almost discrete levels where the energy is practically independent with respect to k_x and k_y. After comparing the structure of subbands originating from different levels it is clearly seen that the internal structure of splitted Landau level varies with the respect to level number N, namely, the total level splitting decreases and the position of clustering point moves to the higher energies.

It should be stressed that the spectrum on Fig.1 is obtained for periodic potential (2) which sign is a constant defined by V_0. Thus, our spectrum differs from those for periodic potential of the form $V(x,y) = V_0 (\cos 2\pi x/a + \cos 2\pi y/a)$ where for energy dependence with respect to q/p one gets a Hofstadter butterfly scaled by Laguerre polynomial L_N[1]. Considering the more realistic potential of quantum dots (antidots) (2), one obtains the energy spectrum (versus q/p) which significantly differs from Hofstadter butterfly. When the condition $V_0 < \hbar\omega_c$ is satisfied, we can use the approximation of non-interactive Landau levels and thus study the splitting of each level independently, neglecting the summation over N in (5). The corresponding matrix equation for coefficients $C_n(k_x,k_y)$ can be written as

$$\frac{1}{2} e^{ik_x a \frac{q}{p}} \left[e^{-\frac{\pi q}{2p}} L_N\left(\pi \frac{q}{p}\right) + \cos\left(2\pi \frac{q}{p}\left[n + \frac{1}{2}\right] + k_y a \frac{q}{p}\right) e^{-\pi \frac{q}{p}} L_N\left(2\pi \frac{q}{p}\right) \right] C_{n+1} + \\ \frac{1}{2} e^{-ik_x a \frac{q}{p}} \left[e^{-\frac{\pi q}{2p}} L_N\left(\pi \frac{q}{p}\right) + \cos\left(2\pi \frac{q}{p}\left[n - \frac{1}{2}\right] + k_y a \frac{q}{p}\right) e^{-\pi \frac{q}{p}} L_N\left(2\pi \frac{q}{p}\right) \right] C_{n-1} + \\ + e^{-\frac{\pi q}{2p}} L_N\left(\pi \frac{q}{p}\right) \cos\left(2\pi n \frac{q}{p} + k_y a \frac{q}{p}\right) C_n = \varepsilon C_n \tag{6}$$

where cyclic boundary condition $C_{n+p} = C_n$ is assumed and cyclotron energy $\hbar\omega_c$ is excluded. The spectrum of system (6) is shown on Fig.2 for three lowest Landau levels $N = 0, 1, 2$. The representation with respect to reciprocal number of flux quanta q/p provides the information on energy spectrum in wider interval of magnetic fields compared with Fig.1 and thus allows us to visualize the energy spectrum both at low ($q/p \approx 1$, right side of Fig.2) and at high ($q/p \ll 1$, left side of Fig.2) magnetic fields. These results seem to be complementary to those obtained in[3] where the energy spectrum has been studied only at low magnetic fields $q/p > 1$. The spectrum on Fig.2 indicates that at intermediate magnetic fields $0.1 < q/p < 1$ the splitting of Landau levels varies due to non-monotonous behaviour of Laguerre polynomials. For small values of p and q (for example, $q/p = 1/4, 1/3, 1/2, 2/3, \ldots$) the spectrum consists of p relatively wide non-overlapping magnetic subbands while for $q/p \ll 1$ (high magnetic fields) the energy subbands are very narrow in accordance with those shown on Fig.1.

Considering our further studies of magnetooptical transitions from acceptors to conduction band, we should be aware of electron wavefunction behaviour in a single superlattice cell compared with those for acceptor. The typical Bohr radius of shallow acceptor in GaAs $r_A \approx 3nm$ which is much smaller then superlattice period $a = 80nm$. This leads to strong dependence of matrix elements on particular position of acceptor inside the superlattice cell. On Fig.3 we show the wavefunctions for two magnetic subbands marked by arrows on Fig.1 which originate from the lowest Landau level. Fig.3a corresponds to the 4th subband located in the region of subbands clustering and Fig.3b is plotted for the 20th (highest) subband. For simplicity we show only the positive values of real part of wavefunction. Hereafter the darker areas on contourplots are related to greater values of wavefunctions. The circle on Fig.3a illustrates relative scale of acceptor and electron wavefunctions. One can clearly see that their overlapping crucially depends on the position of acceptor and the influence of this overlapping on matrix elements will be studied in Sec. IV.

III. HOLE QUANTUM STATES IN THE PRESENCE OF LATERAL SUPERLATTICE AND MAGNETIC FIELD

A. Hole Landau quantum states in p- type heterojunction without periodic potential

We now consider the upper fourfold edge of GaAs p- like valence band at $\mathbf{k} = 0$. Its bulk band structure in the presence of a magnetic field applied in $\langle 001 \rangle$ direction (hereafter denoted by z) is described in axial approximation in terms of 4×4 effective Luttinger Hamiltonian[17,18]

$$H_L = \begin{bmatrix} H_{11} & \overline{\gamma}\sqrt{3}(eH/c)a^2 & \gamma_3\sqrt{6eH/c}\, k_z a & 0 \\ & H_{22} & 0 & -\gamma_3\sqrt{6eH/c}\, k_z a \\ & & H_{33} & \overline{\gamma}\sqrt{3}(eH/c)a^2 \\ & & & H_{44} \end{bmatrix}, \tag{7}$$

where

$$H_{11} = -(\gamma_1/2 - \gamma_2)k_z^2 - (eH/c)\left[(\gamma_1 + \gamma_2)\left(a^+a + \frac{1}{2}\right) + \frac{3}{2}\kappa\right],$$
$$H_{22} = -(\gamma_1/2 + \gamma_2)k_z^2 - (eH/c)\left[(\gamma_1 - \gamma_2)\left(a^+a + \frac{1}{2}\right) - \frac{1}{2}\kappa\right],$$
$$H_{33} = -(\gamma_1/2 + \gamma_2)k_z^2 - (eH/c)\left[(\gamma_1 - \gamma_2)\left(a^+a + \frac{1}{2}\right) + \frac{1}{2}\kappa\right],$$
$$H_{44} = -(\gamma_1/2 - \gamma_2)k_z^2 - (eH/c)\left[(\gamma_1 + \gamma_2)\left(a^+a + \frac{1}{2}\right) - \frac{3}{2}\kappa\right],$$

and the lower half of the matrix is obtained by Hermitian conjugation. Here atomic units $\hbar = m_0 = 1$ are used and the hole energy is measured as negative, e is a module of elementary charge,

$\overline{\gamma} = (\gamma_2 + \gamma_3)/2$, H stands for magnitude of magnetic field, a^+ and a are harmonic oscillator raising and lowering operators. The band parameters appearing in matrix (7) are taken from[18]: $\gamma_1 = 6.85$, $\gamma_2 = 2.1$, $\gamma_3 = 2.9$, and $\kappa = 1.2$. The Luttinger Hamiltonian (7) is written in a basis of p- like atomic functions $v_j(\mathbf{r})$ which transform as a set of eigenfunctions for angular momentum operator $J = 3/2$. These $|J; m_J\rangle$ basis fuctions may be written as following:

$$\begin{cases} v_1 = |\,\frac{3}{2}; \frac{3}{2}\rangle = \left|-\sqrt{1/2}(x+iy)\uparrow\right\rangle, \\ v_2 = |\,\frac{3}{2}; -\frac{1}{2}\rangle = \left|-\sqrt{1/6}(x-iy)\uparrow - \sqrt{2/3}z\downarrow\right\rangle, \\ v_3 = |\,\frac{3}{2}; \frac{1}{2}\rangle = \left|\sqrt{1/6}(x+iy)\downarrow - \sqrt{2/3}z\uparrow\right\rangle, \\ v_4 = |\,\frac{3}{2}; -\frac{3}{2}\rangle = \left|-\sqrt{1/2}(x-iy)\downarrow\right\rangle, \end{cases} \tag{8}$$

where the arrows indicate z-projection of spin.

The holes in GaAs/AlGaAs p- type heterojunction grown in z direction which is parallel to the magnetic field are confined by potential $V_h(z)$ which is a smoothly varying function with triangular shape. It should be noted that such a shape does not have inversion symmetry, i.e. $V_h(z) \neq V_h(-z)$ which leads to the breakdown of twofold spin degeneracy and to the splitting of energy levels of effective Hamiltonian

$$H_{eff} = H_L(a^+, a, k_z) + V_h(z) \tag{9}$$

even at the absence of magnetic field[18]. The lack of inversion symmetry of the atomic potential of GaAs crystal lattice is present also in bulk material and is described by linear k-terms in Luttinger Hamiltonian. However, the effects caused by these terms (the displacement of subbands maxima in $\mathbf{k}$-space[19,20]) are neglegible compared with those induced by heterostructure potential and thus are not considered here.

The solution of the effective-mass equation with Hamiltonian (9) in each of two materials constituting the heterojunction may be written as a four-componenet vector of envelope functions in $|J; m_J\rangle$ basis (8). As it was shown by Luttinger[17], in the presence of magnetic field and under axial approximation one can distinguish the eigenstates of operator (9) by discrete quantum number n which defines the particular set of Landau quantum states. These states have k_y-component of momentum under Landau gauge (3) and in the presence of heterostructure potential the k_z-component is replaced by operator $k_z = -i\partial/\partial z$. Hence, the eigenstate F_{nk_y} of operator (9) consists of four envelope functions $c_j(z)$, $j = 1, 2, 3, 4$[18] and the hole wavefunction is written as

$$\Psi_{nk_y} = \sum_{j=1}^{4} F_{jnk_y} v_j \tag{10}$$

where v_j is a $|J; m_J\rangle$ basis function. Here one can write

$$F_{nk_y} = \left(c_1(z)\phi_{n-2,k_y},\ c_2(z)\phi_{n,k_y},\ c_3(z)\phi_{n-1,k_y},\ c_4(z)\phi_{n+1,k_y}\right). \tag{11}$$

In Eq.(11) $\phi_{nk_y}(x, y) = e^{ik_y}u_n(x)$ is Landau quantum state, and envelope functions $c_j(z)$ vanishe for negative indexes n. For example, for $n = -1$ one can obtain $F_{-1} = (0, 0, 0, c_4(z)\phi_0)$, for $n = 0$ the solution $F_0 = (0, c_2(z)\phi_0, 0, c_4(z)\phi_1)$, and for $n \geq 2$ all four components of (11) will be nonzero. It should be noted that the particular classification of solutions F_n may be chosen in a different way[16] which leads to changes in notation only.

We first observe that for $H = 0$ the Hamiltonian (9) becomes diagonal with elements

$$H_h = -(\gamma_1/2 - \gamma_2)\frac{d^2}{dz^2} + V_h(z),$$
$$H_l = -(\gamma_1/2 + \gamma_2)\frac{d^2}{dz^2} + V_h(z)$$

that yields an infinite set of doubly degenerate heavy and light hole subband energies and eigenfunctions $c_{\nu j}(z), \nu = 1, 2, \ldots$ These functions are usually obtained by solving Schrödinger and Poisson equations self-consistently. As a result, the shape of potential $V(z)$ has a varying gradient which reflects the changes in electric field inside the heterojunction[16,18]. Thus, the precise shape of functions $c_{\nu j}(z)$ differs from the one for the case of uniform electric field. However, the investigations of energy spectrum and matrix elements of transitions between 2D Bloch quantum states and impurities require only the information on overlapping between different localized functions $c_{\nu j}(z)$, and between them and well-known wavefunctions of impurities. The intervals of localization for $c_{\nu j}(z)$ can be obtained with high accuracy for all subbands of size quantization considered in this paper since the shape of $V(z)$ in single GaAs/AlGaAs heterojunction is well-known and was taken by us from[18].

For non-zero magnetic field we have a fan chart of Landau levels originating from each level of size quantization and therefore it is possible to construct the envelope functions for finite H as

$$F_{jk_y} = \sum_{\nu_j n_j} C_{j\nu_j n_j} \phi_{n_j k_y} c_{j\nu_j}. \tag{12}$$

After substituting the function (12) into Schrödinger equation with Hamiltonian (9) one obtaines an algebraic eigenvalue problem for coefficients $C_{j\nu_j n_j}$. We restrict ourself to the first three levels of size quantization which corresponds to consideration of two heavy- and one light-hole levels. This approximation seems to be valid in heterojunctions with typical hole concentration $n = 5 \times 10^{11} cm^{-2}$ and depletion-layer density $N_{dep} = 10^{15} cm^{-3}$ where only the lowest hole level is occupied[18,16]. For each level of size quantization we take into account several Landau levels shown on Fig.4. Here one can see the electron-like behaviour of light-hole Landau levels at low magnetic field caused by proximity of second heavy-hole subband. We assume that the introduction of periodic potential with amplitude V_0 (see the following Subsec.) does not change $c_{\nu j}(z)$ significantly since $|V_0|$ considered in our paper is much smaller then size quantization energies. Hence, in our further studies we use matrix elements of effective Hamiltonian (9) calculated for the functions $c_{\nu j}(z)$ and size quantization energies from[18].

B. Bloch quantum states in the presence of lateral surface superlattice

The problem of hole quantum states in a p- type heterojunction subjected into magnetic field and affected by lateral superlattice is described by Scrödinger equation with vector potential (3) and periodic potential of lateral superlattice given by (2). The Hamiltonian of this problem is a sum of (9) and (2):

$$H = H_{eff} + V(x, y) \cdot E, \tag{13}$$

where E being a unit 4×4 - matrix. The eigenvectors of operator (13) are envelope functions written in $|J; m_J\rangle$ basis (8). The crucial statement here is the following: as long as periodoc potential (2) is applied, every hole envelope function becomes a Bloch function (in the presence of magnetic field) in (xy) plane and is classified by k_x and k_y quantum numbers. Hence, one can write the eigenvector $\Psi^{envelope}_{k_x k_y}(\mathbf{r})$ of operator (13) as

$$\Psi^{envelope}_{k_x k_y}(\mathbf{r}) = \left(\psi^{(1)}_{k_x k_y}(\mathbf{r}),\ \psi^{(2)}_{k_x k_y}(\mathbf{r}),\ \psi^{(3)}_{k_x k_y}(\mathbf{r}),\ \psi^{(4)}_{k_x k_y}(\mathbf{r})\right), \tag{14}$$

and the four-component hole wavefunction is

$$\Psi_{k_x,k_y}(\mathbf{r}) = \psi^{(1)}_{k_x k_y}(\mathbf{r}) \left|\frac{3}{2}; \frac{3}{2}\right\rangle + \psi^{(2)}_{k_x k_y}(\mathbf{r}) \left|\frac{3}{2}; -\frac{1}{2}\right\rangle + \psi^{(3)}_{k_x k_y}(\mathbf{r}) \left|\frac{3}{2}; \frac{1}{2}\right\rangle + \psi^{(4)}_{k_x k_y}(\mathbf{r}) \left|\frac{3}{2}; -\frac{3}{2}\right\rangle. \tag{15}$$

It should be mentioned that the translational properties of each component of envelope function (14) are the same as for electron wavefunction (5). In particular, (14) satisfies to Peierls condition (4). Hence, the hole envelope function may be written in the form

$$\psi^{(j)}_{k_x k_y}(\mathbf{r}) = \frac{1}{La\sqrt{q}} \sum_{S_j} c_{S_j}(z) \sum_{N_j} \sum_{n=1}^{p} G_{jS_jN_jn}(k_x,k_y) \sum_{l=-L/2}^{L/2} u_{Nj}\left(\frac{x-x_0-lqa-nqa/p}{\ell_H}\right) \times$$
$$\times \exp\left(ik_x\left[lqa+\frac{nqa}{p}\right]\right) \exp\left(2\pi i y \frac{lp+n}{a}\right) \exp(ik_y y), \quad (16)$$

where for particular $|J;m_J\rangle$ projection j we summerize over size quantization levels S_j, over Landau levels N_j and over magnetic subbands n. Then, analogous to the electron problem desribed in Sec. II, after substituting the wavefunction (15) into Schrödinger equation with Hamiltonian (13) one obtains the eigenvalue problem for coefficients $G_{jS_jN_jn}(k_x,k_y)$ and hole magnetic subbands $\varepsilon_{jS_jN_jn}(k_x,k_y)$:

$$\sum_{j'S'_jN'_jn'} \left(H^{j'S'_jN'_jn'}_{jS_jN_jn} + V^{j'S'_jN'_jn'}_{jS_jN_jn}(p/q,k_x,k_y)\right) G_{j'S'_jN'_jn'} = \varepsilon G_{jS_jN_jn}. \quad (17)$$

Here the notation $H^{j'S'_jN'_jn'}_{jS_jN_jn}$ is used for projection of Hamiltonian (9) onto our basis (j S_j N_j n) and $V^{j'S'_jN'_jn'}_{jS_jN_jn}(p/q,k_x,k_y)$ stands for matrix elements of periodic potential (2) calculated in this basis. The spectrum of system (17) at the center of magnetic Brilloin zone $k_x = k_y = 0$ is shown of Fig.5 for the case of non-overlapped subbands related to the highest hole levels $n = 2+$ and $n = -1-$. Here the sign $+(-)$ refers to the spin projection of dominating component of $|J;m_J\rangle$ basis[18,16]. Similar to the electron spectrum shown on Fig.1, every hole Landau level has splitted into p narrow magnetic subbands grouped near the unperturbed level. The condition $|V_0| \leq \Delta E_{12}$ where ΔE_{12} is the distance between levels $n = 2+$ and $n = -1-$ allows to observe the set of non-overlapped magnetic subbands for these levels at high magnetic fields.

It was mentioned previously that hole Landau levels may be classified into groupes of effective Hamiltonian (13) eigenvalues labeled by common index $n = -1, 0, 1, \ldots$ For example, for $n = 0$ such group belonging to subband of size quantization with $\nu = 1$ consists of one heavy-and one light-hole level. These levels can be obtained by diagonalization of 2×2 matrix and are labeled by $n = 0-(+)$ (see Fig.4). When the periodic potential of lateral superlatice is introduced, the 2×2 matrix yields $2p \times 2p$ matrix equation (17) which spectrum consists of $2p$ magnetic subbands originating from $n = 0-(+)$ levels. If the amplitude $|V_0|$ is small enough to neglect the influence of other levels neighbouring with the levels $n = 0-(+)$, it is possible to study their splitting separately. The set of $2p$ magnetic subbands originating from levels $n = 0-(+)$ splitted by periodic potential with $V_0 = -3meV$ is shown on Fig.6a(b). Note that in subbands originating from $n = 0-$ level (Fig.6a) the heavy-hole component with angular momentum $m_J = -3/2$ dominates in the wavefunction while in subbands splitted from $n = 0+$ level (Fig.6b) the light-hole component with $m_J = -1/2$ has the biggest amplitude. Comparing Fig.2 and Fig.6, one can see that the difference between electron and hole spectrum increases at high magnetic fields $q/p \ll 1$ where the off-diagonal element of Luttinger Hamiltonian $\gamma_3\sqrt{6eH/c}\ k_z a$ becomes more significant.

In the following Sec. we will calculate the matrix elements for transitions between valence band and donors located in heterojunction and thus the knowledge of hole wavefunction in superlattice cell is required. The real part of hole wavefunction component $m_J = -3/2$ which dominates among four components of hole wavefunction (15) in Landau state $n = -1-$ is shown on Fig.7 at $k_x = k_y = 0$. This picture is plotted for subbands 181 and 200 which are marked by arrows on Fig.5. As for electron quantum states, in subband 181 located far from the clustering point, the wavefunction (Fig.7a) has much less zeros then for subband 200 belonging to the region of subbands clustering (Fig. 7b). In detail, the real part of hole wavefunction on Fig.7a lays below zero almost everywhere and has a sharp minimum at $x = y = 0$. On the opposite, the values of wavefunction for subband 200 shown on Fig.7b are distributed more uniformly above and below zero and thus

Fig.7b has less dark areas then Fig.7a. We've not shown the contourplots for imaginary part of wavefunction since they demonstrate the same behaviour. One can expect that the discussed difference in wavefunction shape should be reflected in magnitude of matrix elements for transitions to donors and it will be proved in the following Sec.

When the condition $|V_0| < \Delta E_{12}$ is not fulfilled, the structure of hole spectrum looks different. The spectrum for $V_0 = -10meV$ and $\Delta E_{12} \approx 2.5meV$ is shown on Fig.8. In this case magnetic subbands originating from different hole Landau levels are strongly overlapped almost everywhere except the region near the highest Landau level. This region is marked on Fig.8 and it containes magnetic subbands from 209 to 220 belonging to Landau level $n = 2+$. In this interval of non-overlapping subbands one may expect a distinguishible behaviour of magnetooptical matrix elements for these subbands (see the following Sec).

Under the conditions of strong subbands overlapp the domination of one of $|J; m_J\rangle$ basis component becomes less pronounced. This is illustrated on Fig.9 where all four $|J; m_J\rangle$ components of wavefunction are shown for subband 185 marked by arrow on Fig.8. It is clearly seen that all components have the same order which is a consequence of overlapping of those magnetic subbands originating from Landau levels with different dominating wavefunction components.

IV. MATRIX ELEMENTS FOR TRANSITIONS BETWEEN CONDUCTION (VALENCE) BAND AND ACCEPTORS (DONORS)

As it was mentioned in the Introduction, one of possible experimental tools for investigation of quantum states in magnetic subbands are magnetooptical measurements of transition intensities. Below we calculate the matrix elements between Bloch quantum states and impurities located in heterojunction subjected to magnetic field.

First of all we consider a process in which photon is absorbed and electron is raised from acceptor atom to electron quantum state (1) described in Sec. II. It is supposed that the monolayer of aceptors is located at well-defined distance from heterojunction interface[15,16]. The initial quantum state $\Psi^I_{x_0y_0}$ is a wavefunction of shallow acceptor localized at (x_0, y_0) point in $z = z_0$ plane and it has the envelope function of the form

$$\psi_{x_0y_0} = A \exp\left(-\frac{1}{r_A}\left[\varrho^2 + (z - z_0)^2\right]^{1/2}\right), \tag{18}$$

where A is normalizing constant, $\varrho^2 = (x - x_0)^2 + (y - y_0)^2$, $r_A = \kappa_e\hbar^2/m_{val}e^2$ is Bohr radius of acceptor, κ_e is the dielectric constant of material. Here m_{val} stands for averaged effective mass at the top of valence band with p - type atomic function $p(\mathbf{r})$. We believe that both atomic and envelope functions in Eq.(18) are practically unaffected by external magnetic field. The parameters for which the matrtix elements of transitions between acceptors and conduction band have been calculated were the following: $p/q = 20$ (corresponding to $H \approx 12.1\ T$), the amplitude of periodic potential $V_0 = 20\ meV$ and $a = 80\ nm$. In this case the set of non-overlapping magnetic subbands has a simple structure shown on Fig.1. For direct optical transitions one can write[21]

$$\begin{aligned} M_{k_xk_y}(x_0, y_0) = \langle \Psi^F_{k_xk_y} \mid \mathbf{p}\cdot\mathbf{e} \mid \Psi^I_{x_0y_0}\rangle = \\ = \langle s \mid \mathbf{p}\cdot\mathbf{e} \mid p\rangle\langle\psi_{k_xk_y} \mid \psi_{x_0y_0}\rangle + \mathbf{e}\cdot\langle\psi_{k_xk_y} \mid \mathbf{p} \mid \psi_{x_0y_0}\rangle\langle s \mid p\rangle, \end{aligned} \tag{19}$$

where $\mathbf{e}$ being a unit vector in the direction of incident electric field and scalar products are defined as

$$\langle s \mid (\ldots) \mid p\rangle = \int_{cell} s^*(\mathbf{r})(\ldots)p(\mathbf{r})d\mathbf{r},$$

$$\langle\psi_{k_xk_y} \mid (\ldots) \mid \psi_{x_0y_0}\rangle = \int_{crystal} \psi^*_{k_xk_y}(\mathbf{r})(\ldots)\psi_{x_0y_0}(\mathbf{r})d\mathbf{r}.$$

The first term in (19) corresponds to matrix elements of interband transitions from acceptors to conduction band while the second one has a form of intraband transitions which occur at cyclotron resonance[4]. For the problem which is under consideration in this paper the latter term vanishes due to ortogonality of atomic functions $p(\mathbf{r})$ and $s(\mathbf{r})$ being p- and s - type functions, respectively. The uniform distribution of space orientation for p - type acceptor atomic functions is assumed and one can easily check that due to this fact the matrix element $\langle s \mid \mathbf{p}\cdot\mathbf{e} \mid p\rangle$ in (19) does not depend on polarization of incident radiation.

In Sec. II it was found that the overlapping of electron and acceptor wavefunctions and thus the matrix element strongly depend on the position of acceptor atom in a current superlattice cell. In order to obtain the transition probability for lateral superlattice with many cells we have to average it over many possible acceptor positions:

$$\overline{\mid M \mid^2_{k_x k_y}} = \frac{1}{N_A} \sum_{x_0, y_0} \mid M_{k_x k_y}(x_0, y_0) \mid^2, \tag{20}$$

where N_A is total number of acceptor positions. It should be noted that due to the random position of acceptor atom the matrix elements do not depend on the quasimomentum which classify the Bloch quantum state (5). This independance on k_x and k_y reflects the behaviour of electron wavefunctions which practically remain unchanged with respect to the variations of quasimomentum. On Fig.10 we plot the averaged square of matrix element module which determines the transition probability to the particular subband of Landau levels shown on Fig.1. In order to compare these values with matrix element for unperturbed Landau level we plot this matrix element multiplied by p (being the ratio between the number of states per Landau level and per one magnetic subband) on the left side of each histogramm of Fig.10 (marked as LL). The elements from 1st to 20th (Fig.10a) correspond to transitions to the lowest Landau level $N = 0$, the elements from 21st to 40th (Fig.10b) are plotted for the level $N = 1$ and the elements from 81st to 100th (Fig.10c) describe the transitions to the level $N = 4$. Looking on Fig.10 one can see the huge increase of matrix elements with respect to subband number inside one Landau level. It reflects the distribution of electron wavefunction shown on Fig.3: wavefunction in subbands which are located near clustering point (Fig.3a) have more oscillations (more zeros) then those related to other edge of splitted Landau level (Fig.3b). By comparing Fig.10a(b) and Fig.10c one can see the decrease of matrix elements magnitude both for unperturbed Landau level (marked as LL) and for magnetic subbands in which it has been splitted in. One may expect that such a decrease is caused by increasing number of wavefunction oscillations with respect to Landau level index N.

The calculation of matrix elements for valence band – donors transitions can be investigated similarely to the problem of acceptors – conduction band trabsitions discussed above. Namely, the initial quantum state $\Psi^I_{k_x k_y}$ is now a hole wavefunction (15), and the final quantum state Ψ^F is wavefunction of shallow donor impurity located in the layer $z = z_0$ and described by envelope function $\psi_D(\mathbf{r})$

$$\psi_D = A \exp\left(-\frac{1}{r_D}\left[\varrho^2 + (z - z_0)^2\right]^{1/2}\right),$$

where analogous to (18) $r_D = \kappa_e \hbar^2 / m_{eff} e^2$ stands for donor Bohr radius (its typical value is $\approx 15nm$) and m_{eff} is effective mass at the bottom of conduction band. This band is characterized by s- type atomic function $s_\alpha(\mathbf{r})$ where the index $\alpha = 1(2)$ corresponds to the function $\mid s \uparrow\rangle$ ($\mid s \downarrow\rangle$). Since the total ansamble of donor atoms does not have definite projection of angular momentum, one can write

$$\Psi^F = \psi_D \frac{\mid s \uparrow\rangle + \mid s \downarrow\rangle}{\sqrt{2}}.$$

After the definition of initial and final quantum states, we write the matrix element similiar to (19) as

$$M_{k_x k_y} = \langle \Psi^F \mid \mathbf{p}\cdot\mathbf{e} \mid \Psi^I_{k_x k_y} \rangle =$$

$$= \sum_{\alpha=1}^{2}\sum_{j=1}^{4} \langle s_\alpha \mid \mathbf{p}\cdot\mathbf{e} \mid v_j \rangle \langle \psi_D \mid \psi^{(j)}_{k_x k_y} \rangle + \sum_{\alpha=1}^{2}\sum_{j=1}^{4} \mathbf{e}\cdot \langle \psi_D \mid \mathbf{p} \mid \psi^{(j)}_{k_x k_y} \rangle \langle s_\alpha \mid v_j \rangle, \tag{21}$$

where v_j is $|J; m_J\rangle$ basis function (8) and the second term in (21) again vanishes. On the opposite to the electronic case, the hole – donor transition intesities strongly depend on polarizatoin of incident radiation. On the one hand, it is a consequence of different contribution of $|J; m_J\rangle$ basis components into hole quantum state (15) and, on the other hand, the transitions from heavy holes are three times more intensive then those from light holes (see, for example,[21,15]). The z-dependent calculation of integral $\langle \psi_D \mid \psi^{(j)}_{k_x k_y} \rangle$ is performed for functions $c(z)$ for typical GaAs/AlGaAs heterojunction taken from[18]. Similar to the case of transitions between acceptors and conduction band, we have to average the matrix elements over many possible donor positions. The averaged squares of matrix elements module (21) calculated for two highest Landau levels $n = -1-$ and $n = 2+$ being splitted by $V_0 = -2.5meV$ are shown on Fig.11. Here Fig.11a(b) corresponds to $\sigma^+(\sigma^-)$ polarized radiation. It is evident that magnetic subbands related to different hole Landau levels exhibit itself differently. Namely, for σ^+ polarization the matrix elements for subbands 181 – 200 related to $n = -1-$ level are two orders of magnitude larger then those related to $n = 2+$ level. On the contrary, for σ^- polarization the elements for subbands 201 – 220 related to $n = 2+$ are five orders of magnitude larger then the elements corresponding to $n = -1-$ level. We believe that such drastic differences in magnetooptical parameters will provide more transparence in experimental studies of hole magnetic subbands. It is obvious that the low amplitude of periodic potential $|V_0| < \Delta E_{12}$ is important for non-overlap of magnetic subbands which is illustrated on Fig.12 where matrix elements for the same Landau levels $n = -1-$ and $n = 2+$ splitted by higher periodic potential of quantum dots $V_0 = -10meV$ are shown. The switching of polarization from σ^+ (Fig.12a) to σ^- (Fig.12b) leads to total decrease of matrix elements but their internal shape changes significantly mainly for subbands 209 – 220 which are not overlapped with those related to other Landau levels (see the marked region on Fig.8). The polarization switching illuminates these subbands and thus makes possible to detect them experimentally.

V. SUMMARY AND CONCLUSIONS

We investigated quantum states and magnetooptics of 2D electrons and holes in heterojunctions subjected to perpendecular magnetic field and periodic potential of superlattice. The electron quantum states in n-type heterojunction have been studied both for coupled and uncoupled Landau levels in a wide interval of magnetic field. The holes in p-type heterojunction were described by 4×4 Luttinger Hamiltonian where both confinement potential and potential of lateral surface superlattice have been introduced. This model allowed us to figure out the influence of spin-orbit coupling onto four-component Bloch quantum states in external magnetic field. We've calculated hole magnetic subbands at high magnetic fields under consideration of several Landau levels originating from the first three subbands of size quantization. In a wider interval of both low and high magnetic fields the set of hole magnetic subbands originating from two coupled Landau levels has been obtained. Here the increasing differences with electron quantum states occure at high magnetic fields which is caused by the H-dependent off-diagonal term in Luttinger Hamiltonian. Then the calculations of matrix elements for transitions between electron magnetic subbands and acceptors and between hole magnetic subbands and donors have been performed. We found the characteristic dependencies of matrix elements on subband number both in n- and p-type heterojunctions. In the latter case the strong dependence on polarization of incident radiation is found. In particular, at σ^+ (σ^-) polarization the most intensive transitions are from those hole magnetic subbands where "spin"-down(up) components of wavefucntion dominate. The discussed effects allowed us to define the set of parameters (superlattice periods, amplitude of periodic potential and magnetic field value) for transparent experimental observation of sharp non-overlapping magnetic subbands both for electrons and holes.

ACKNOWLEDGMENTS

We thank A.A. Perov for fruitful discussions and for technical assistance. This work was supported by the Russian Foundation of Basic Research (Grant No. 01-02-17102), by the Russian Ministry of Education (Grant No. E00-3.1-413) and jointly by CRDF Foundation and Russian Ministry of Education (Project No. REC - 001).

---

[1] D.J. Thouless *et al.*, Phys. Rev. Lett. **49**, 405 (1982).
[2] H. Silberbauer, J. Phys.: Condens. Matter **4**, 7355 (1992).
[3] D. Springsguth, R. Ketzmerick, and T. Geisel, Phys. Rev. B **56**, 2036 (1997).
[4] V.Ya. Demikhovskii and A.A. Perov, Phys. Low-Dim. Structures **7/8**, 135 (1998).
[5] N. Usov, Sov. Phys. JETP **67**, 2565 (1988).
[6] P.B. Wiegman and A.V. Zabrodin, Phys. Rev. Lett. **72**, 1890 (1994).
[7] Y. Hatsugai, M. Kohmoto, and Y.S. Wu, Phys. Rev. Lett. **73**, 1134 (1994); Phys. Rev. B **53**, 9697 (1996).
[8] I. Krasovsky, Phys. Rev. B **59**, 322 (1999).
[9] J. Eroms *et al.*, Phys. Rev. B **59**, R7829 (1999).
[10] G. Petscel and T. Geisel, Phys. Rev. Lett. **71**, 239 (1993).
[11] R. Ketzmerick *et al.*, Phys. Rev. Lett **84**, 2929 (2000).
[12] D. Weiss *et al.*, Phys. Rev. Lett. **66**, 27 (1991).
[13] T. Schlösser *et al.*, Semicond. Sci. Technol. **11**, 1582 (1996); Europhys. Lett. **33**, 683 (1996).
[14] C. Albrecht *et al.*, Phys. Rev. Lett. **86**, 147 (2001).
[15] I.V. Kukushkin *et al.*, Phys. Rev. Lett. **79**, 1722 (1997).
[16] O.V. Volkov *et al.*, Phys. Rev. B **56**, 7541 (1997).
[17] J.M. Luttinger, Phys. Rev. **102**, 1030 (1956).
[18] D.A. Broido and L.J. Sham, Phys. Rev. B **31**, 888 (1985).
[19] Yu.A. Bychkov and E.I. Rashba, in the *Proc. of the* 17th *Int. Conf. on the Phys. Semicond.*, San Francisco (1984), Springer Verlag (1985), p. 321.
[20] G.E. Marques and L.J. Sham, Surf.Sci. **113**, 131 (1982).
[21] F. Ancilotto, A. Fasolino, and J.C. Maan, Phys. Rev. B **38**, 1788 (1988).

arXiv:cond-mat/0112465v1 [cond-mat.mes-hall] 27 Dec 2001

Figure captions

V.Ya. Demikhovskii and D.V. Khomitsky

"Quantum states and optics in n - and p -type heterojunctions with lateral surface quantum dot (antidot) superlattice subjected to perpendicular magnetic field"

Fig.1. Electronic spectrum versus magnetic flux p/q in antodot lattice with $a = 80\ nm$ and $V_0 = 20\ meV$ at high magnetic fields. Magnetic subbands for three splitted Landau levels $N = 0$, $N = 1$, and $N = 4$ (on the inset) are shown together with positions of unperturbed levels (dark circles).

Fig.2. Electron spectrum versus reciprocal magnetic flux q/p in antidot lattice with $a = 80\ nm$ and $V_0 = 2\ meV$ shown for the model of non-interactive Landau levels $N = 0, 1, 2$ on Fig.2 (a) – (c), respectively.

Fig.3. Electron wavefunctions (positive values of real part) in one cell of antidot superlattice for two magnetic subbands marked by arrows on Fig.1 which originate from the lowest Landau level $N = 0$. Fig.3a corresponds to the 4th subband located in the region of subbands clustering and Fig.3b is plotted for the 20th (highest) subband. Darker areas indicate higher values of function module. The circle on Fig.3a illustrates relative scale of acceptor and electron wavefunctions.

Fig.4. Set of hole Landau levels corresponding to first three subbands of size quantization (two heavy- and one light-hole levels). The electron-like behaviour of light-hole Landau levels at low magnetic field can be observed. Each level is characterized by Landau index $n = -1, 0, 1, \ldots$ and by dominating spin projection $\pm$ (see text). Hereafter the energy is measured from the top of valence band in bulk GaAs.

Fig.5. Non-overlapped hole magnetic subbands related to the highest hole levels $n = 2+$ and $n = -1-$. The amplitude of quantum dots potential $V_0 = -2.5meV$.

Fig.6. Hole energy spectrum in quantum dots lattice with $a = 80nm$ versus reciprocal magnetic flux q/p shown for two hole levels $n = 0 - (+)$ coupled by off-diagonal elements of Luttinger Hamiltonian and splitted by periodic potential with $V_0 = -3meV$.

Fig.7. Real parts of envelope hole wavefunctions (component $m_J = -3/2$) in one superlattice cell at $k_x = k_y = 0$ for subbands 181 (Fig.7a) and 200 (Fig.7b) marked by arrows on Fig.6.

Fig.8. Hole energy spectrum for $V_0 = -10meV$ and $p/q = 20$. Magnetic subbands originating from different hole Landau levels are strongly overlapped almost everywhere except the marked region (subbands from 209 to 220) near the highest Landau level $n = 2+$.

Fig.9. Four components of hole envelope wavefunction ($Re\psi_j > 0$) at $k_x = k_y = 0$ for subband 185 marked by arrow on Fig.8. The figures from (a) to (d) correspond to the components $|\ \frac{3}{2}; \frac{3}{2}\rangle$, $|\ \frac{3}{2}; -\frac{1}{2}\rangle$, $|\ \frac{3}{2}; \frac{1}{2}\rangle$ and $|\ \frac{3}{2}; -\frac{3}{2}\rangle$ of $|J; m_J\rangle$ basis, respectively.

Fig.10. Averaged square of matrix element module determining the probability of transitions between acceptors and the particular electron magnetic subband. Hereafter the subband number is counted on x axis for levels $N = 0$ (subbands 1 – 20), $N = 1$ (21 – 40) and $N = 4$ (81 – 100). The squared matrix element for transitions to unperturbed Landau level (marked as LL) multiplied by number of magnetic subbands $p = 20$ is plotted on the left side of each histogramm.

Fig.11. Averaged square of matrix element module for transitions between hole magnetic subbands and donors for two highest Landau levels $n = -1-$ and $n = 2+$ splitted by periodic potential with $V_0 = -2.5meV$. Fig.11a(b) corresponds to σ^+ (σ^-) polarization.

Fig.12. Averaged square of matrix element module for transitions between hole magnetic subbands and donors for two highest Landau levels $n = -1-$ and $n = 2+$ splitted by periodic potential with $V_0 = -10meV$ and for σ^+ (Fig.12a) and σ^- (Fig.12b) polarization. The switching of polarization from σ^+ to σ^- leads to total decrease of matrix elements but their internal shape changes significantly mainly for subbands 209 – 220 which are not overlapped with those related to other Landau levels (see the marked region on Fig.8).